ELSEVIER

Physica A 241 (1997) 278–283

PHYSICA A

Recent advances in strong field magneto-transport in a composite medium

David J. Bergman [a,*], Yakov M. Strelniker [a], Andrey K. Sarychev [b]

[a] *School of Physics and Astronomy, Raymond and Beverly Sackler Faculty of Exact Sciences, Tel Aviv University, Tel Aviv 69978, Israel*

[b] *Scientific Centre of Applied Problems in Electrodynamics, Russian Academy of Sciences, Izhorskaya 13/19, Moscow 127412, Russia*

Abstract

Macroscopic inhomogeneities have a profound effect on electrical conductivity in the presence of a strong magnetic field **B**. One expression of this is the appearance of a new physical length in the system, which increases with **B** and is unbounded. This length characterizes the extra distortions of the local current density which are produced by the strong Hall effect. In fractal clusters, different scaling behavior is found to occur at scales above and below this length. In random percolating systems, the new length competes with the percolation correlation length for dominance over the critical behavior. The divergence of each of these lengths is associated with a different fixed point. In metallic composites with a periodic microstructure, the new length is responsible for a strong anisotropy which appears in the magneto-resistance, even when the rotational symmetry is simple cubic or simple square.

PACS: 72.15.Gd; 05.70.Jk
Keywords: Optics; Microwaves; Dielectric constant; Percolation

In the presence of a strong magnetic field **B**, even a simple, free electron metal in the regime of classical, macroscopic transport has its electrical properties altered significantly by the appearance of a Hall field. The resistivity becomes a non-symmetric tensor ($\omega_c \equiv e|\mathbf{B}|/mc$ is the electron cyclotron frequency, τ is the conductivity relaxation time)

$$\mathbf{E} = \hat{\rho}\mathbf{J}, \quad \hat{\rho} = \rho_0 \begin{pmatrix} 1 & -H & 0 \\ H & 1 & 0 \\ 0 & 0 & 1 \end{pmatrix} \text{ for } \mathbf{B} \,\|\, z\,, \tag{1}$$

* Corresponding author. Fax: 97236422979; e-mail: bergman@post.tau.ac.il.

PII S0378-4371(97)00095-2

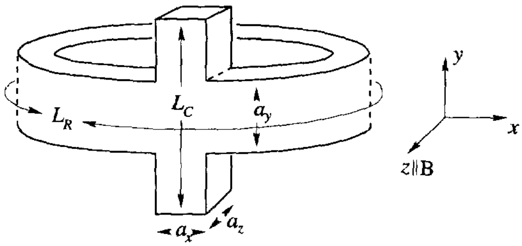

Fig. 1. Chain and ring device for demonstrating how Hall effect can lead to magneto-resistance.

$$H \equiv \frac{\rho_{\mathrm{Hall}}}{\rho_{\mathrm{Ohmic}}} = \pm\,\omega_c\tau \propto |\mathbf{B}|\,. \tag{2}$$

In a uniform system, where $\hat{\rho}$, $\mathbf{J}$, $\mathbf{E}$ are position-independent, the Hall resistivity does not contribute to energy dissipation, because $\mathbf{J}$ is determined by the boundary conditions while the $\mathbf{B}$-dependent component of $\mathbf{E}$ is perpendicular to $\mathbf{J}$. However, when the system is macroscopically non-uniform, $\mathbf{J}$ is non-uniform even when $\mathbf{B}=0$, and its spatial configuration is further altered when $\mathbf{B}\neq 0$. This produces extra dissipation, which depends on $\mathbf{B}$ and has the effect of making the bulk effective Ohmic resistivity (i.e., the symmetric part of the bulk effective resistivity tensor $\hat{\rho}_e$) $\mathbf{B}$-dependent, in contrast with the Ohmic components of $\hat{\rho}$ in the case of a uniform free electron metal.

A simple configuration where these effects can be demonstrated is the chain and ring device shown in Fig. 1. If the conductor cross sections are all small compared to the chain length L_C and ring circumference L_R, then we can describe the electrical properties by assuming uniform current densities J_C, J_R in both the chain and the ring. The value of J_C is determined by the boundary conditions, while J_R is determined by the requirement that the line integral of $\mathbf{E}$ around the ring must vanish. In this way, the total dissipation is found to be (ρ is the Ohmic resistivity while $H\rho$ is the Hall resistivity of the chain and ring material)

$$\rho J_R^2 \left(a_x a_z L_C + H^2 \frac{a_y^3 a_z}{L_R} \right). \tag{3}$$

The second term can be interpreted as an increase $\delta\rho$ in the Ohmic resistivity, where

$$\frac{\delta\rho}{\rho} = \frac{a_y^3 H^2}{L_C L_R a_x}\,. \tag{4}$$

Since we assumed that $a_x, a_y, a_z \ll L_C, L_R$, this induced magneto-resistance will only be appreciable if H is large enough. The expression we got shows the importance of parameters like L/a, where L is a typical conductor length and a is a typical conductor thickness: aH defines a length scale in the system such that if $L \leqslant aH$ then $\delta\rho/\rho$ is appreciable.

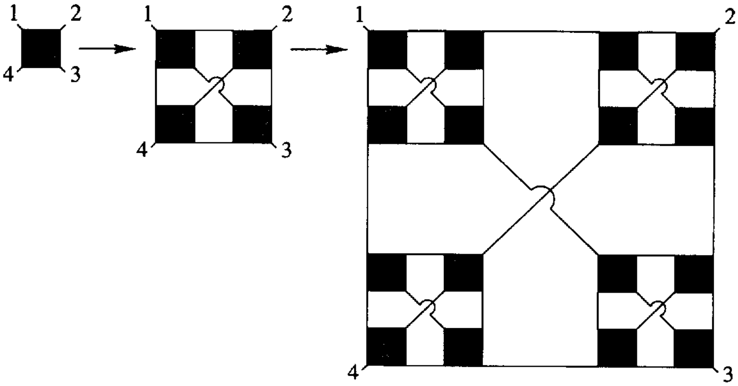

Fig. 2. The first three generations of a three-dimensional Sierpiński gasket network, where at each vertex is placed a replica of the four terminal device shown on the left as the first generation and described by (5) and (6). Each of the gray squares can be thought of as a metallic tetrahedron, viewed from a direction that is perpendicular to two non-intersecting edges.

The most important element in the above discussed system can be described as a discrete four terminal device, where currents I_j and voltages V_i can be applied at each terminal (see Fig. 2). These currents and voltages are related by

$$V_i = \sum_{i=1}^{4} R_{ij} I_j \,, \tag{5}$$

$$R_{ij} = \frac{1}{2} R(\delta_{ij} + H Y_{ij}), \quad \hat{Y} = \begin{pmatrix} 0 & -1 & 0 & 1 \\ 1 & 0 & -1 & 0 \\ 0 & 1 & 0 & -1 \\ -1 & 0 & 1 & 0 \end{pmatrix} . \tag{6}$$

When such elements are connected together in a regular fractal array, like the three-dimensional Sierpiński gasket (see Fig. 2), the result is a solvable model where the electrical properties can be calculated in detail at all scales [1]. An important conclusion is that there is a critical length scale $\xi_H = aH^{\nu_H}$, where $\nu_H = 1/[\ln(\sqrt{2}+2)/\ln 2 - 1] \cong 1.296$ and a is the size of an elementary tetrahedron: On length scales $L \gg \xi_H$ the current distribution is the same as it would be at $H = 0$, and only its absolute magnitude depends upon H. By contrast, on length scales $L \ll \xi_H$ the current distribution is totally different from the $H = 0$ configuration. However, the distribution as well as the absolute magnitudes of those currents are saturated – they do not change even when H is increased further.

A real space renormalization group transformation, as well as computer simulations, applied to a percolating random network model where each element is similar to the device described in (5) and (6) but now has six terminals, leads to qualitatively similar conclusions [2]. In addition to the percolation correlation length ξ_p, which has a

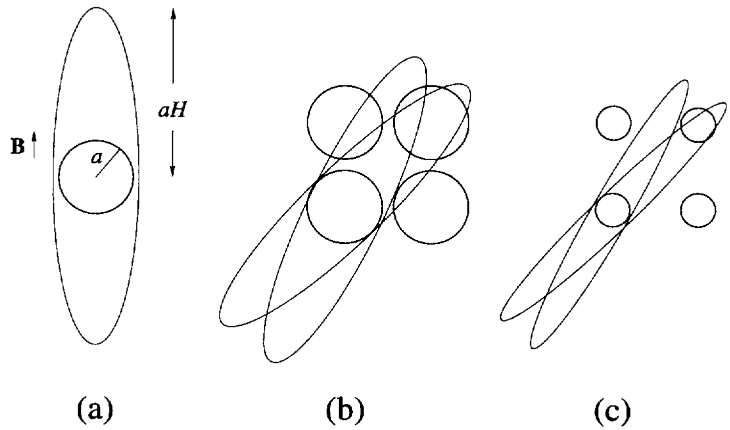

Fig. 3. (a) Cigar-shaped region of strong current distortion near a spherical inclusion. (b) and (c) Arrays of inclusions with different inclusion sizes: In (c) the distortion cigar can clearly reach the next nearest neighbor without obstruction, but not in (b).

geometric significance and diverges at the percolation threshold, there now appears a magnetic-field-dependent length $\xi_H \propto H^{\nu_H}$, $\nu_H \cong 0.5$. Two fixed points now compete for control of the critical behavior: When $\xi_p \gg \xi_H$, the $H = 0$ fixed point governs that behavior and the critical exponents assume their "weak (magnetic) field values". By contrast, when $\xi_p \ll \xi_H$, the $H = \infty$ fixed point governs that behavior and the critical exponents assume a different set of "strong field values".

A field-dependent length also appears when just a single compact inclusion of linear size a is embedded in an otherwise homogeneous free electron metal. A current density that is uniform far away from the inclusion gets distorted in its vicinity. When $H \gg 1$ (H refers to the host, not the inclusion), then the region of strong distortion has the shape of a cigar with its long axis parallel to **B**, cross section equal to that of the inclusion, and length equal to aH [3] (see Fig. 3(a)). The current distortion results in extra dissipation which is saturated deep inside this region. Therefore, the total extra dissipation is approximately proportional to H. This linear dependence on H will begin to saturate when the distortion region encounters distortion regions from other inclusions.

For a random, isotropic distribution of such inclusions, this results in a positive magneto-resistance that is independent of the direction of **B**, and is proportional to $|\mathbf{B}|$ as long as $a \ll aH \ll 1/n^{1/3}$, where n is the average number density of the inclusions. For higher fields the magneto-resistance will begin to saturate. However, for an ordered periodic array of inclusions, a magneto-resistance will appear that can oscillate quite strongly with changes in the direction of **B**. In Fig. 4 the circles show results of measurements of the resistivity of a doped GaAs thin film in which a periodic, square array of holes was punched, when a strong magnetic field is applied in different directions in the film plane [4]. Both the longitudinal and the transverse relative magneto-resistance of these composite films ($\delta\rho_{\parallel}$ and $\delta\rho_{\perp}$, respectively) show a strong

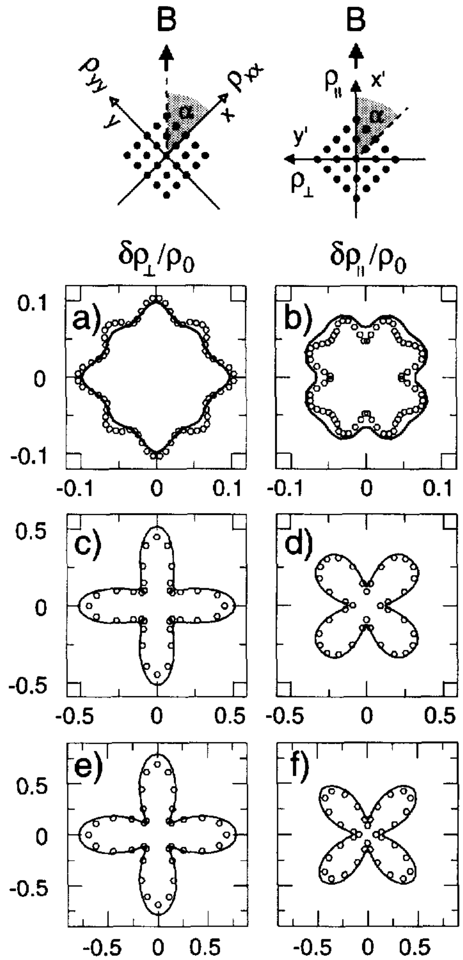

Fig. 4. Polar plots of $\delta\rho_\perp(\mathbf{B})/\rho_0$ and $\delta\rho_\parallel(\mathbf{B})/\rho_0$ for three samples of Si-doped GaAs thin films (thickness $\approx 300\,\text{Å}$) with a square array (lattice parameter $b \approx 500\,\text{Å}$) of approximately cylindrical holes and different hole radii a: From top to bottom $a/b = 0.146, 0.360, 0.430$. The magnetic field was 12 T, which corresponds to $H \cong 3$ for these samples. Circles indicate measured values, lines were calculated by solving (7), using a/b as fitting parameter (after Ref. [4]).

dependence on the direction of **B**. The measurements were performed under conditions where quantum and ballistic effects are negligible (i.e., temperature $T = 90\text{K}$, and mean free path much smaller than hole sizes or separations). The entire phenomenon could be described by classical macroscopic physics, i.e., by solving the stationary continuity equation in order to find the static electric potential field $\phi(\mathbf{r})$:

$$\nabla \cdot [\hat{\sigma}(\mathbf{r})\nabla\phi(\mathbf{r})] = 0\,, \tag{7}$$

where $\hat{\sigma}(\mathbf{r}) = 1/\hat{\rho}(\mathbf{r})$ is the local conductivity tensor. Such calculations are not easy to perform when $H \gg 1$, but efficient methods for doing them have been developed [5–7].

The results of such a calculation are also shown in Fig. 4 as solid lines. The oscillations of $\delta\rho/\rho_0$ (ρ_0 is the Ohmic resistivity of the uniform film, which is independent of **B**) with changing direction of **B** are due to the complex interferences and interactions between the current distortions produced by different inclusions.

Some features of the oscillation patterns can be understood from a simple geometric shadow picture of those interactions: The interactions become important as soon as the cigar-shaped region of strong distortion produced by a single obstacle begins to overlap with a similar region produced by another obstacle. This happens when aH is equal to the nearest-neighbor distance *in the direction of* **B**. Such an interaction can either enhance or attenuate the extra dissipation, depending on whether the two distortion patterns interfere constructively or destructively – this is the reason for the different behavior of $\delta\rho_\perp$ and $\delta\rho_\parallel$ which is evident in Fig. 4 [4,8].

The distortion patterns from two inclusions can only interact in a simple way if no other inclusions intrude upon the two cigar-shaped regions of strong distortions. Such intrusions will always occur if the two inclusions are sufficiently far apart, or if they and the other inclusions are sufficiently large (see Figs. 3(b) and (c)). That is why for an array of very large inclusions, only distortions from nearest neighbors are able to interact and lead to strongly oscillatory behavior. When the inclusion size a is decreased, then distortions from further neighbors can also interact, but this requires a larger value of H (see Fig. 3(c)). This explains why for smaller inclusions more oscillations of $\delta\rho$ are observed with changing direction of **B**, but this requires a larger magnitude $|\mathbf{B}|$ (see Fig. 4).

Acknowledgements

This research was supported in part by grants from the Israel Science Foundation and the US–Israel Binational Science Foundation.

References

[1] A.K. Sarychev, D.J. Bergman and Y.M. Strelniker, Phys. Rev. B 48 (1993) 3145.
[2] A.K. Sarychev, D.J. Bergman and Y.M. Strelniker, Europhys. Lett. 21 (1993) 851.
[3] C. Herring, J. Appl. Phys. 31 (1960) 1939.
[4] M. Tornow, D. Weiss, K.v. Klitzing, K. Eberl, D.J. Bergman and Y.M. Strelniker, Phys. Rev. Lett. 77 (1996) 147.
[5] D.J. Bergman and Y.M. Strelniker, Phys. Rev. B 49 (1994) 16256.
[6] Y.M. Strelniker and D.J. Bergman, Phys. Rev. B 50 (1994) 14001.
[7] D.J. Bergman and Y.M. Strelniker, Phys. Rev. B 51 (1995) 13845.
[8] Y.M. Strelniker and D.J. Bergman, Phys. Rev. B 53 (1996) 11051.